Effect of Pore-Wall Chemistry on Proton Conductivity in Mesoporous Titanium Dioxide

Flávio Maron Vichi, M. Isabel Tejedor-Tejedor, and Marc A. Anderson*

Water Chemistry Program, University of Wisconsin−Madison, 660 N. Park St., Madison, Wisconsin 53706

Received November 30, 1999. Revised Manuscript Received March 2, 2000

In this paper we describe how the conductivity of a mesoporous TiO_2 membrane is strongly affected by the chemistry of the pore walls. We have studied the effect of site density, state of surface protonation, and surface modification in samples with a fixed pore structure. Pore structure was kept fixed by firing all samples at the same temperature. Changing the surface site density (number of water molecules per square nanometer) from 5.5 to 5.7 leads to an increase in conductivity from 8.00×10^{-3} to 1.00×10^{-2} Ω^{-1} cm^{-1} at 25 °C and 81% relative humidity (RH). The effect of the state of protonation was studied by pretreating wafers at pH 1.5 and equilibrating them with solutions at pH 2.5 and 4.0. This variable (protonation state of the material) was found to have an even stronger effect on conductivity. Surface modification was achieved by adsorbing phosphate anions from solutions with different pH. It was observed that even a very small degree of phosphate loading (0.71 ions/nm^2) leads to an increase in conductivity from 8.27×10^{-3} to 9.66×10^{-3} Ω^{-1} cm^{-1} at pH 2.5. The conductivity of our materials, especially those treated at pH 1.5, is very close to that of Nafion, a polymeric material used as a proton conducting membrane in fuel cell systems. The lower cost and higher hydrophilicity of our materials make them potential substitutes for costlier hydrophobic polymeric membranes in fuel cells.

Introduction

Perfluorosulfonic polymers[1] currently serve as electrolytes in proton exchange membrane (PEM) fuel cells due to their high protonic conductivity at low temperature. The protonic conductivity of these polymers under high (80%) relative humidity (RH) ranges between 2.8×10^{-2} Ω^{-1} cm^{-1} for Nafion 117[2] to 8.8×10^{-2} Ω^{-1} cm^{-1} for Dow membranes.[1,3] Presently, Nafion is one of the few materials that deliver the set of chemical and mechanical properties required to perform as a good PEM.[4] The conductivity of Nafion increases with increasing RH (at room temperature, the conductivity for Nafion at 81% RH is 1 order of magnitude higher than it is at 31% RH [2]) but does not improve significantly with increasing temperature.[5] This behavior has been attributed to the inability of this perfluorosulfonic polymer to retain water at higher temperatures and limits the fuel cell operation to ∼80 °C. In addition to this restriction, Nafion membranes are very expensive.

If one wishes to improve upon the commercial potential of PEM fuel cells, the development of new proton-conducting materials is imperative. Future materials should provide high proton conductivity at low temperature; they should be hydrophilic and mechanically, thermally, and chemically stable; they also should be impermeable to H_2 and O_2.

Over the last 10 years, the proton conductivity characteristics of porous ceramic films of metal oxides have been the subject of growing interest due to their potential as humidity sensors. Binary and ternary mixtures of TiO_2 with other oxides such as Al_2O_3, SnO_2, and V_2O_5 sintered at high temperature (about 1000 °C) display conductivity values from 10^{-11} to 10^{-5} Ω^{-1} cm^{-1} in the range of 15−95% RH, at 25 °C.[6] Although these values are much lower than those observed for Nafion, we believe that this is largely due to the low specific surface area (below 1 m^2/g); low porosity (≤30% porosity); large pore diameters (ranging from teens of nanometers to micrometers); and loss of hydrophilicity due to the high extent of surface dehydroxylation in these porous ceramic films. In this regard, the effect of sintering temperature on the protonic conductivity of SiO_2 has been correlated to changes in pore structure.[7] In a recent publication,[8] we have shown that under the right conditions, proton conductivity for porous SiO_2 and TiO_2 materials can reach values similar to that of Nafion.

As discussed above, TiO_2 has been shown[8] to have potential as an electrolyte in PEM fuel cells. It has a

* To whom correspondence should be addressed. E-mail: nanopor@facstaff.wisc.edu. Fax: (608) 262-0454.

(1) Gottesfeld, S.; Zawodsisnki, T. A. Polymer Electrolyte Fuel Cells. In *Advances in Electrochemical Science and Engineering*; Alkire, R. C., Gerischer, H., Kolb, D. M., Tobias, C. W., Eds.; Wiley-VCH: Weinheim, 1997; Chapter 5, pp 245−263.

(2) Summner, J. J.; Creager, S. E.; Ma, J. J.; DesMarteau, D. D. *J. Electrochem. Soc.* **1998**, *145*, 107.

(3) Zawodsisnki, T. A.; Neeman, M.; Sillerud, L.; Gottesfeld, S. *J. Phys. Chem.* **1991**, *95*, 6040.

(4) Kreuer, K. D. *Solid State Ionics* **1997**, *97*, 1.

(5) Sone, Y.; Ekdunge, P.; Somonsson, D. *J. Electrochem. Soc.* **1996**, *143*, 1254.

(6) Traversa, E. *Sens. Actuators B* **1995**, *23*, 135.

(7) Nogami, M.; Nagao, R.; Wong, C. *J. Phys. Chem. B* **1998**, *102*, 5772.

(8) Vichi, F. M.; Colomer, M. T.; Anderson, M. A. *Electrochem. Solid State Lett.* **1999**, *2*, 313.

10.1021/cm9907460 CCC: $19.00
Published on Web 04/27/2000

proton conductivity similar to that of Nafion; it can be fabricated as thin (submicron) porous ceramic films with pore size below 30 Å; it is highly insoluble in acid solution; and it is thermally stable below 400 °C. Our research is aimed at optimizing the proton conductivity of this material. For this purpose we are studying how physical and chemical changes in this material influence its proton conductivity. As in the case of Nafion, our earlier studies[8] have unveiled that when the RH changes from 33 to 81%, the conductivities of porous Al_2O_3, TiO_2, and SiO_2 increase by orders of magnitude. Therefore, it is important to determine the primary variables controlling water adsorption in these mesoporous metal oxide ceramics.

It is well-known that for any given adsorbate, pore structure and surface chemistry of the adsorbent will determine the shape of the adsorption isotherm. In the particular case of water, adsorption in pores smaller than 10 nm diameter has been described as a two-regime process. At low and moderate relative pressures, water molecules first adsorb directly onto acidic and basic surface sites, on which further water molecules adsorb via hydrogen bonding, leading to the formation of a layer of water clusters.[9−11] With increasing relative pressure, the water layer thickens and consequently causes an increase in the interlayer curvature that leads to capillary condensation. McCallum and co-workers[9] propose a different pore filling mechanism for water adsorption in nanopores of activated carbon. Their model predicts that water clusters, on the same wall and/or opposing walls, will be connected through bridging water molecules. The model also predicts that these molecules will act as nuclei for further adsorption, eventually leading to pore filling. In the context of this model, materials with a large surface site density may reach pore filling by a continuous process without capillary condensation. It has been shown that the value for the capillary condensation pressure not only depends on the pore size, as predicted by the Kelvin equation, but also on the chemistry of the pore wall.[11−14]

In summary, the structure and surface chemistry of the pore wall will determine the degree of hydration of nanoporous materials for a given set of RH and temperature conditions. In this particular paper, we will study the influence of the surface chemistry on the proton conductivity of TiO_2 ceramic wafers having a given porous structure that does not change in the process of modifying the surface.

It is known that the surface of titanium dioxide has both Lewis acid (five-coordinated Ti^{4+} ions) and basic (two-coordinated O^{2-}) sites. Water can be adsorbed on the five-coordinated Ti^{4+} ions in a molecular and/or in a dissociated form.[15−17] The dissociative adsorption process involves an acidic site which binds the water molecule and a basic site which abstracts the proton resulting in the formation of singly coordinated and doubly coordinated surface hydroxyls. Henderson et al.[15] have shown a correlation between the proclivity to undergo dissociative adsorption and the proximity between acidic and basic sites for different crystal planes. Although the mechanism for water adsorption on TiO_2 remains a subject of controversy, there is general understanding that surface structure (crystalline phase and exposed crystallographic planes)[15−17] and defects will determine whether the process is molecular or dissociative in nature and also the quantity of water adsorbed. Water can also be physisorbed through hydrogen bonding on both hydroxyl and molecular water surface groups.

The heat treatment of a TiO_2 xerogel determines not only its pore structure (surface area, pore size, and pore volume) but also the crystal structure of TiO_2, the size of the microcrystalline domain, and the degree of surface oxygenation.[18] These properties are all expected to influence, as mentioned above, the water adsorption behavior of this porous material.[19] These parameters were held constant for this study by using a single heat treatment for all samples, while varying the nature of the chemical groups on the pore wall. We intend to modify the ratio of five-coordinated Ti^{4+}/two-coordinated O^{2-} groups by treating the porous TiO_2 with an acidic solution at pH 1.5. We will also change the state of surface protonation by equilibrating this material with aqueous solutions of different pH. In addition, we will alter the surface by phosphate adsorption. These changes are aimed at investigating the influence of surface site density, charge density, as well as surface acidity and interfacial dipolar charge distribution on the water adsorption of TiO_2.

The nature of the surface groups is expected to influence the protonic conductivity not only by affecting the water adsorption behavior of the material but also by influencing the mobility of protons in water clusters. Water structure, as determined by hydrogen bonding, mobility, and polarization, is perturbed by the presence of the pore walls. The degree of perturbation is connected with the magnitude and distribution of the interfacial charge.[20] Proton mobility, on the other hand, is mainly governed by proton hopping and in some degree by the hydrodynamic proton mobility.[21] Stronger hydrogen bonds result in a *loss* of hydrodynamic mobility (self-diffusion) and, up to a limit, in an increase of proton hopping frequency.

We will determine the effect of the nature of surface groups in the mobility of protons in the water clusters.

Experimental Section

Synthesis of the Wafers. A porous xerogel of TiO_2 was prepared by the controlled drying of the precursor sol. The TiO_2 sol was synthesized by the hydrolysis of titanium isopropoxide and dialyzed following the procedure of Xu and Anderson.[18] To fabricate xerogels with flat crack-free regions larger than 1 cm^2, the sol was dried in Teflon dishes at 25 °C and at

(9) McCallum, C. L.; Bandosz, T. J.; McGrother, S. C.; Müller, E. A.; Gubbins, K. E. *Langmuir* **1996**, *12*, 533.
(10) Salame, I. I.; Bagreev, A.; Bandosz, T. J. *J. Phys. Chem. B* **1999**, *103*, 3877.
(11) Salame, I. I.; Bandosz, T. J. *Langmuir* **1999**, *15*, 587.
(12) Llewellyn, P. L.; Schüth, F.; Grillet, Y.; Rouquerol, F.; Rouquerol, J.; Unger, K. K. *Langmuir* **1995**, *11*, 574.
(13) Zhu, H. Y.; Ni, L. A.; Lu, G. Q. *Langmuir* **1999**, *15*, 3632.
(14) Burkat, T. M.; Semashko, O. V.; Us'yarov, O. G. *Colloid J.* **1999**, *61*, 284.
(15) Henderson, M. A. *Langmuir* **1996**, *12*, 5093.
(16) Bredow, T.; Jug, K. *Surf. Sci.* **1995**, *327*, 398.
(17) Stefanovich, E. V.; Truong, T. N. *Chem. Phys. Lett.* **1999**, *299*, 623.
(18) Xu, Q.; Anderson, M. A. *J. Mater. Res.* **1991**, *6*, 1074.
(19) Franke, M. E.; Simon, U. *Solid State Ionics* **1999**, *118*, 311.
(20) Marrink, S.-J.; Berkowitz, M.; Berendsen, H. J. C. *Langmuir* **1993**, *9*, 3122.
(21) Agmon, N. *J. Chim. Phys.* **1996**, *93*, 1714.

constant RH. The sol was gelled rapidly (generally after 48 h) under low-RH conditions (20−40%) to minimize pore size in the xerogel. The resulting gel was then left for 1 week to dry slowly at ambient conditions (25 °C, 45% RH). To fabricate the porous ceramics used as sample specimens in this study, the dry xerogel was fired at 400 °C for 3 h, yielding ceramic wafers with thicknesses ranging from 0.1 to 0.13 cm. We will refer to this material as Ti400.

Surface Modification. To study the effect of surface protonation on conductivity, at a constant site density (five-coordinated Ti^{4+}/bridging O^{2-}), Ti400 wafers were placed in small Teflon screen baskets, which were immersed for 24 h in a stirred HNO_3 solution at pH 1.5, yielding material Ti1.5. Samples of this material were then rinsed with water and left to equilibrate for 24 h with HNO_3 solutions of constant pH 2.5 and 4.0. After equilibration, the samples were dried at 60 °C for 12 h prior to conductivity measurements. We will refer to these samples as Ti1.5−2.5 and Ti1.5−4.0, respectively. All treatments were performed at room temperature.

To study the effect of site density on proton conductivity, Ti400 wafers were also treated with HNO_3 solutions at pH 2.5 and 4.0 for 24 h, without pretreatment at pH 1.5. These samples will be referred to as Ti2.5 and Ti4.0, respectively.

Pore surface modification with orthophosphate was achieved by adsorption at equilibrium from aqueous solution. Ti400 wafers were left to equilibrate, at 23 °C, with milimolar KH_2PO_4 solutions, 0.01 M KNO_3 ionic strength, for 24 h. The adsorptions were performed at pH 2.5 and 4. The pH was adjusted to the desired value with HNO_3 and kept constant during the adsorption process. The amount of adsorbed phosphate was calculated by the difference between the initial concentration of the solution and the concentration after reaching equilibrium. The concentration of phosphate left in solution was measured by ion-coupled plasma spectrometry using a Perkin-Elmer Plasma II spectrometer. The quantity of phosphate adsorbed was 158 μmol/g at pH 2.5 (TiP2.5) and 53 μmol/g at pH 4.0 (TiP4.0). To examine the effect of pH on the conductivity of phosphated samples, the TiP4.0 wafer was subsequently treated at pH 2.5 for 24 h, yielding sample TiP4.0−2.5.

Characterization Methods: Pore Size and Surface Area. The pore structures and the specific surface areas of the Ti400 wafers were determined by N_2 adsorption/desorption isotherm analysis using a Micromeritics ASAP 2000 surface area analyzer. Pore size distribution calculations were based on the Kelvin equation and the BJH method.

Chemisorbed Water. The number of hydroxyl groups per unit area of the samples was measured by thermogravimetric analysis (TGA) using a Netzsch STA 409 system. This analysis was performed on samples of Ti400, Ti1.5, Ti2.5, and Ti4.0 and an unfired xerogel (which we will call TXG). All these materials were exposed for several days to 81% RH to reach full surface hydroxylation/hydration before performing the TG analysis. The TG curves were registered under static dry air atmosphere and the following heating program: the temperature was increased to 60 °C at a rate of 1 °C min^{-1} and dwelled at 60 °C for 6 h. Next, the temperature was increased to 350 °C at a rate of 2 °C min^{-1}. The weight loss before 100 °C is assigned to physisorbed water, and the loss between 100 and 350 °C to surface hydroxyl groups and/or coordinated H_2O.

Water Adsorption Isotherms. Physisorbed water in all these materials was measured at 15, 25, and 40 °C as a function of RH. In this experiment, samples were kept in a closed thermostatic chamber with the desired RH maintained by saturated solutions of the appropriate salts [$MgCl_2 \cdot 6H_2O$ for 33%, $NaI \cdot 2H_2O$ for 38%, $Mg(NO_3)_2 \cdot 6H_2O$ for 53%, NaBr for 58%, NH_4NO_3 for 62%, NaCl for 75%, $(NH_4)_2SO_4$ for 81% and KNO_3 for 92% RH]. Samples were left to equilibrate at each RH and temperature until constant weight was observed. Generally, equilibrium was reached after 24 h. With the help of a robotic arm, the weight of the equilibrated samples was measured using a Mettler AT 261 Delta Range balance placed inside the chamber.

Protonic Conductivity. This property was measured by Electrochemical Impedance Spectroscopy (EIS). Alternate current (ac) impedance spectra were collected using a HP-4192A frequency response analyzer (FRA), in the frequency range of 5−10 MHz and oscillating voltage of 50 mV and a Solartron SI 1260 FRA in the frequency range 50−32 MHz and the same oscillating voltage. The spectra were analyzed using the EQUIVCRT program by Boukamp[22] and Z-Plot for Windows.

The specimens for these measurements were flat wafers of the above-mentioned porous ceramic materials ~0.1 cm thick. Gold electrodes (area: 0.28 cm^2) were sputtered onto both sides of each wafer, and the samples were placed in Teflon sample holders having spring-loaded Pt contacts. Prior to collecting impedance spectra, the wafers were allowed to equilibrate at the desired RH (33, 38, 51, 58, 62, 75, and 81%) and temperature for 24 h in sealed chambers containing saturated solutions of the above-mentioned appropriate salts. Constant temperature was obtained by immersing the sample chambers in a water bath.

The reproducibility of the results was verified by repeating the measurements three times for a given sample, and also by testing different samples of the same material equilibrated under the same conditions. Variation between different measurements with the same sample is less than 0.5%, and between similar measurements with different samples was also less than 0.5%.

Results and Discussion

Surface Area and Pore Structure. The N_2 adsorption/desorption isotherm for Ti400 wafers is of type IV, and exhibits an E type hysteresis loop. These results are indicative of a mesoporous material with mainly cylindrical pore shape, and rather narrow pore size distribution. The BET surface area is 134 $m^2\ g^{-1}$, the BJH desorption average pore diameter is 49.7 Å, and the BJH desorption cumulative pore volume is 0.236 $cm^3\ g^{-1}$.

Chemisorbed Water. Unfired xerogels (TXG) and also xerogels sintered at 400 °C (Ti400) and reexposed to water vapor are expected to have molecular water or hydroxyl groups coordinated to surface five-coordinated Ti^{4+} ions and hydroxyl groups coordinated to bridging O^{2-} ions (chemisorbed water). Also, these porous materials should have water molecules hydrogen bonded (physisorbed) to bridging O^{2-} ions of the surface (second layer water) and to other hydrogen bonded water molecules (multilayer water). The adsorption energy for physisorbed water is smaller than for chemisorbed molecular water/hydroxyl groups.[9,11,23] Therefore, physisorbed and chemisorbed water should evolve at different temperatures and, under the right experimental conditions, be discernible by TGA. The TG curves of TXG, Ti400, and Ti2.5 recorded under the conditions reported in the experimental part are shown in Figure 1. TG curves of Ti1.5 and Ti4.0 specimens show the same features as those of Ti400 and Ti2.5. All the curves exhibit a fairly distinct two-step shape. There is a mass loss below 60 °C, followed by a plateau, and a second mass loss starting near 80 °C which continues up to 350 °C. The first loss is ascribed to the physisorbed water (second layer and multilayer) and the second one is attributed to the desorption of both coordinated molecular water (at the lower end of temperature) and water resulting from the recombination of terminal and bridg-

(22) Boukamp, B. Equivalent Circuit (EQUIVCRT.PAS), University of Twente, Twente, The Netherlands, 1988−89.

(23) Wendlandt, W. WM. *Thermal Analysis*; John Wiley & Sons: New York, 1986; p 190.

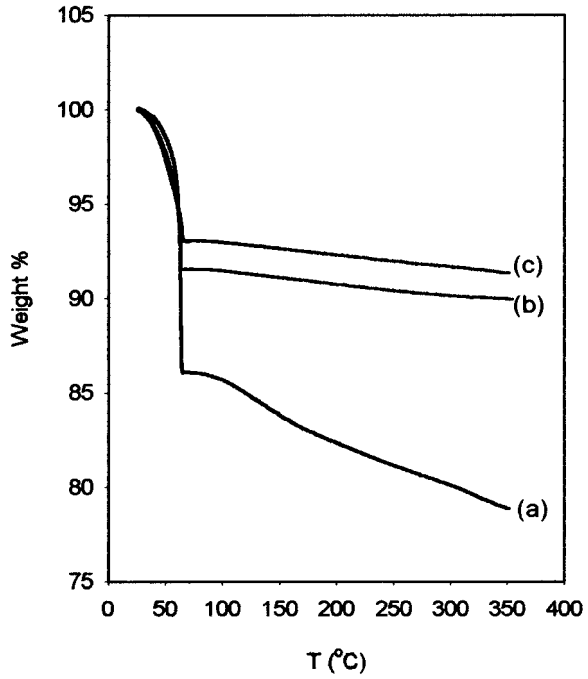

Figure 1. TG curves for materials TXG (a), Ti400 (b), and TiP2.5 (c).

Table 1. Chemisorbed Water in the Samples

sample	% H_2O	molecules/nm^2
TXG	8.9	12.5
Ti400	1.7	5.1
Ti4.0	1.7	5.1
Ti2.5	1.8	5.4
Ti1.5	1.9	5.7

ing surface hydroxyls.[9,23,24] Results from the analysis of the TG curves are reported in Table 1. The data show that the amount of chemisorbed water desorbed from the xerogel (12.5 per nm^2) is 2.4 times larger than for the materials first heated at 400 °C and then reexposed to water vapor (Ti400). In other words 60% of the chemisorbed water of the TXG samples is irreversibly lost upon heating at 400 °C. Moreover, by treating the Ti400 specimen with nitric acid solutions at pH 2.5 (Ti2.5) and 1.5 (Ti1.5) for 24 h, the reversible fraction of this type of water increases, but only by a small percentage (14%).

The maximum quantity of coordinated water available for desorption can be predicted from the theoretical density of five-coordinated Ti^{4+} sites. In a defect-free surface both numbers should coincide. The theoretical density of this type of site for the (110), (101), and (100) surfaces of TiO_2 (rutile) are 5.2, 7.9, and 7.4 sites per nm^2 respectively. Water desorption measurements for powder rutile give 6.2 H_2O molecules per nm^2.[9,25,26] For powder anatase the concentration of surface OH groups, measured by isotopic exchange with D_2O, is 4.9 per nm^2.[27] Therefore, the amount of coordinated water on the surface of Ti400, Ti4.0, Ti2.5, and Ti1.5 specimens (5.1−5.7 molecules/nm^2) is in reasonable agreement with literature data. The larger amount of coordinated water obtained for TGX samples (12.5 molecules/nm^2) is probably related to its amorphous character, which is equivalent to having a very defective structure. It is known that the presence of oxygen defects in a surface increases the density of five-coordinated Ti^{4+} sites.[16]

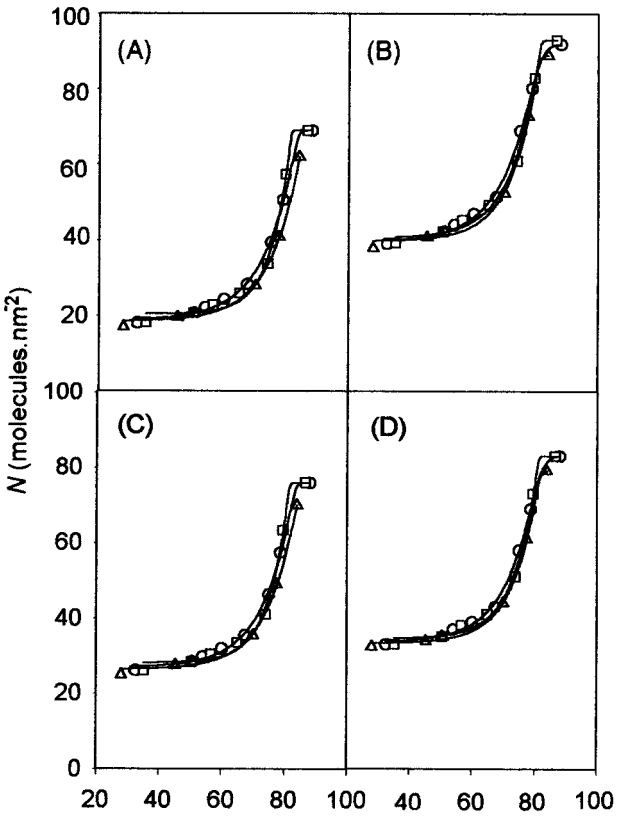

Figure 2. Water adsorption isotherms at 15 (○), 25 (□), and 40 °C (△): (A) Ti400, (B) Ti1.5, (C) TiP4.0, and (D) TiP2.5.

Physisorbed Water. Figure 2 shows water adsorption isotherms on Ti400, Ti1.5, TiP4.0, and TiP2.5 at 15, 25, and 40 °C in terms of water content (number of molecules per square nanometer, *N*) versus RH. These isotherms should be classified as type IV, given the fact the samples are mesoporous materials. The adsorption of water in these samples is totally reversible in the lower pressure range (below 30% RH). Since the outgassing of the samples prior to measuring the isotherms was done at 60 °C, the chemisorbed water was not removed and therefore the isotherms include only physisorbed water. Also, the shape of these isotherms is indicative of porous materials with surface polar groups,[24] as is expected for metal oxides with coordinated water and hydroxyl surface groups. The isotherms in Figure 2 indicate that adsorption at RH below 60% corresponds to the formation of a layer of water clusters and, at a higher RH, to the filling of the pores.

Although all the isotherms shown in Figure 2 belong to samples having the same surface area and pore space, the amount of water adsorbed along the linear part of the isotherm (between 30 and 60% RH) is quite different for the four different materials. However, the amount of water adsorbed by capillary condensation is practically the same for all the materials. Data from the adsorption isotherms are reported in Table 2. These

(24) Gregg, S. J.; Sing, K. S. W. *Adsorption, Surface Area and Porosity*; Academic Press: London, 1982; Chapter 5, p 248.
(25) Jones, P.; Hockey, J. A. *Trans. Faraday Soc.* **1971**, *67*, 2679.
(26) Yates, D. E. Ph.D. Thesis, University of Melboure, Australia, 1975.
(27) Schindler, P. W. Surface Complexes at Oxide−Water Interfaces. In *Adsorption of Inorganics at the Solid−Liquid Interface*; Anderson, M. A., Rubin, A. J., Eds.; Ann Arbor Science Publishers: 1981; Chapter 1, p 5.

Table 2. Physisorbed Water Content (*N*) in the Samples as a Function of RH

	physisorbed *N* (molecules/nm^2)			
% RH[a]	Ti400	Ti1.5	TiP2.5	TiP4.0
35	18	39	33	26
50	21	42	35	28
57	23	45	38	31
65	26	49	41	34
74	34	61	51	41
80	57	83	73	63
87	69	93	83	76

[a] With the use of saturated solutions, RH was determined for each solution using a humidity sensor.

data show existing qualitative differences in the polarity of these adsorbent surfaces[24] and also the extent of their influence on the uptake behavior of water. Following the data in Table 2, changing the protonation state of the pore walls and/or exchanging surface OH/H_2O by other ligands, such as for example orthophosphate ions can cause the sample uptake of physisorbed water to increase up to 100% at partial pressures below 60% RH. Since the uptake by capillary condensation is practically the same for all samples, the total quantity of water at 90% RH is also much higher in the highly surface protonated sample (Ti1.5) than it is in the sample rehydrated by exposure to water vapor (Ti400).

Since surface hydroxyls and water ligands are the major anchor points for physisorption of water molecules,[24] some correlation between the density of five-coordinated Ti^{4+} sites and the amount of water adsorbed in the cluster layer region of the isotherm (linear part below 60% RH) can be expected. However, the monolayer capacities corresponding to chemisorbed and physisorbed water were found to be in the ratio 1:3.9 for the Ti400 and 1:7.1 for Ti1.5. These results show that although the monolayer capacity for physisorbed water should be influenced by the density of five-coordinated Ti^{4+} sites, the latter is not the only variable affecting the former.[19,20,24] Charge density as well as interfacial dipolar charge distribution are expected to influence the size and the structure of the water clusters for a given relative pressure. Since the pH of the isoelectric point is 5.5 for TiO_2, the Ti1.5 specimen should be positively charged. Although Ti400 will still develop a positive charge in the presence of water, this will be much smaller. Preliminary data on phosphate adsorption isotherms for Ti400 indicates that the phosphate coverage in the TiP2.5 sample is a small fraction of a monolayer, therefore its surface will still be very positive at pH 2.5. In the case of TiP4.0, for which the phosphate adsorption density is about one-third of that in sample TP2.5, the water adsorption in the region of the physisorbed water monolayer is unexpectedly high when compared with the Ti400 sample.

The pore volume calculated from the water isotherms varies from 0.275 cm^3 g^{-1} for Ti400 to 0.370 cm^3 g^{-1} for sample Ti1.5. This value is always larger than the one calculated from the N_2 isotherm (0.236 cm^3 g^{-1}). These results suggest that the water in the pores is present in a form more dense (pore water density: 1.16, 1.28, 1.41, and 1.57 g cm^{-3} for Ti400, TiP4.0, TiP2.5, and Ti1.5, respectively) than that of ordinary water.

Conductivity. Electrochemical impedance spectroscopy (EIS) yields slightly depressed semicircles for low-conductivity samples, and inclined lines for the high-conductivity ones, as exemplified in Figure 3. Conductivities at 25 °C for our samples range from 4.93 $\times$ 10^{-6} Ω^{-1} cm^{-1} for Ti400 at 33% RH to 1.95 $\times$ 10^{-2} Ω^{-1} cm^{-1} for Ti1.5 at 92% RH. At room temperature, the conductivity of Nafion reported by Sumner[2] ranges from 1 $\times$ 10$^{-2}\Omega^{-1}$ cm^{-1} at 45% RH to 4 $\times$ 10$^{-2}\Omega^{-1}$ cm^{-1} at 70% RH. At higher temperatures, the conductivity does not increase at the same rate as it does with relative humidity, and the values reported by Sone and co-workers for Nafion at 45 and 80 °C and 80% RH are 1 $\times$ 10^{-2} and 2 $\times$ 10$^{-2}\Omega^{-1}$ cm^{-1}, respectively.[5] Our materials have conductivities which are very close to that of Nafion. Furthermore, we have shown previously[8] that the conductivity of Ti400 increases by a factor of 4 when the temperature is raised from 25 to 80 °C. Assuming that all samples behave similarly, we can expect that the conductivity of Ti1.5 will be higher than that of Nafion at these higher temperatures.

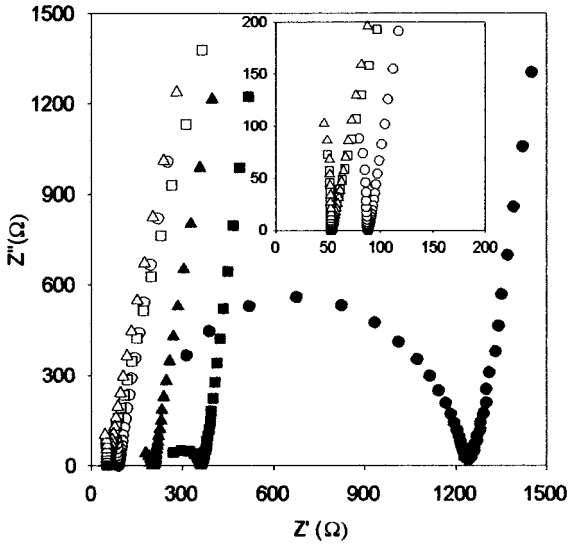

Figure 3. Effect of RH on the impedance spectra of Ti1.5;: (●) 33%, (■) 53%, (▲) 62%, (○) 75%, (□) 81%, and (△) 92%.

The conductivity of our samples depends strongly on sample surface properties, RH and temperature as will be demonstrated shortly. We will analyze separately the influence of each of these variables on sample conductivity.

Influence of the Surface Site Density. Table 1 shows that the density of chemisorbed water molecules and/or single coordinated OH groups (density of five-coordinated Ti^{4+} sites) depends on the conditions under which the parent sample of TiO_2 undergoes rehydration. Whether the wafers are exposed to water vapor (Ti400) or immersed in a water solution at pH 4 does not seem to affect the number of chemisorbed water molecules per unit area (5.1 molecules/nm^2). However, the exposure of the parent sample to water solutions at pH 2.5 and 1.5 increases the density of coordinated water to 5.4 and 5.7 molecules/nm^2, respectively. The influence of site density on proton conductivity is shown in Figure 4, where we compare the conductivity of two wafers, Ti2.5 and Ti1.5−2.5. The first sample is the product of treating a Ti400 wafer with a HNO_3 solution at pH 2.5 and the second one was generated by treating a Ti400 wafer with a HNO_3 solution at pH 1.5 and then letting the new product equilibrate with a HNO_3 solution at

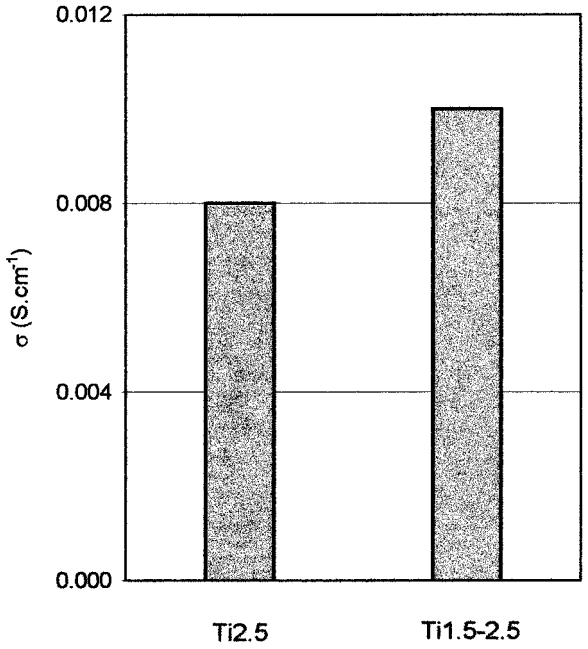

Figure 4. Influence of site density on proton conductivity at 25 °C and 81% RH.

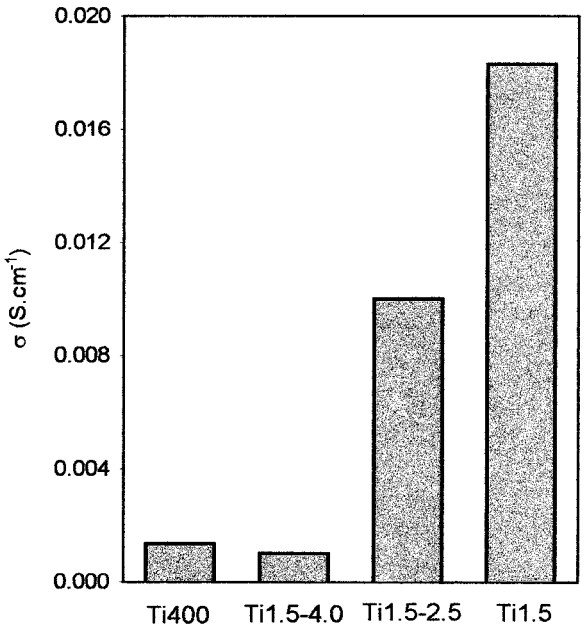

Figure 5. Influence of the state of surface protonation on proton conductivity at 25 °C and 81% RH.

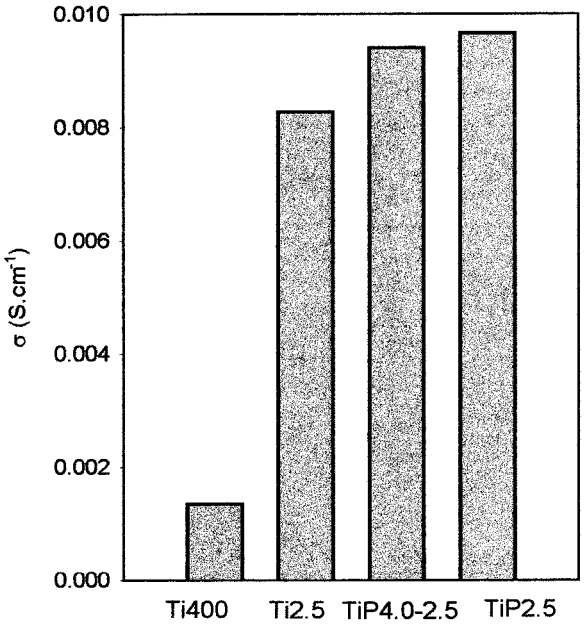

Figure 6. Influence of phosphate adsorption on proton conductivity at 25 °C and 81% RH.

pH 2.5. Therefore, any difference in the state of surface protonation in these samples should come only from having a different surface site density of five-coordinated Ti^+ ions. Data in Table 1 and Figure 4 show that by increasing the density of surface sites by 5%, the conductivity of the TiO_2 improved by 21%.

Effect of the State of Surface Protonation. Ti400 wafers were first treated with a aqueous solution at pH 1.5 (sample Ti1.5) and then left to equilibrate with solutions at pH 2.5 and 4, to yield samples Ti1.5−2.5 and Ti1.5−4, respectively. The pretreatment at pH 1.5 ensures that all three samples have the same site density and should only differ in their state of surface protonation.

Wafers of Ti1.5 immersed in ultrapure water release 4.49 mmol of H^+/g. Three potential sources of these protons could be the surface of the pores, the interfacial double layer, or the bulk solution in the pore, which has a pH of 1.5. Since the bulk water solution in the pores at pH 1.5 can only contain 7.37×10^{-4} mmol of H^+/g, most of the 4.49 mmol/g of protons released by the sample should come from the interfacial region. More specifically, these protons are most likely surface species, since at pH 1.5 the TiO_2 surface is positive and therefore the proton concentration in the double layer should be depleted in relation to the bulk solution in the pore.

Conductivity values for these three samples at 25 °C and 80% RH are reported in Figure 5. In the pH range between 4 and 1.5, the conductivities of the samples increase linearly with decreasing the equilibration pH, following the equation: $\sigma = -0.0068\text{pH} + 0.028$. These changes in sample conductivity as a function of the degree of surface protonation could be justified on several grounds: (1) due to changes in the hydration state of the sample, since, judging from the adsorption isotherms of Figure 2, the degree of sample hydration at a given RH depends largely on the surface chemistry of the pore walls; (2) to differences in the concentration of H^+ ions in the pore; and finally, (3) to divergences in the mobility of those protons which should be affected by the charge of the pore surface. Conversely, in the case of these samples, charge is fixed by its protonation state.

Influence of Phosphate Ions on the Surface. The conductivities for samples equilibrated at pH 2.5 and having different loadings of phosphate ions on the pore walls are reported in Figure 6. The density of phosphate ions on the surface of samples TiP2.5, TiP4.0−2.5, and Ti2.5 is 0.71 ions/nm^2 (158 μmol/g), 0.24 ions/nm^2 (53 μmol/g), and zero, respectively. Figure 6 shows that the presence of phosphate ions on the pore walls increases the conductivity of the samples, although not by a large amount. However, some ongoing experiments suggest that the adsorption density in both samples is very low when compared with the maximum adsorption density expected at these pH values. This is in accordance with

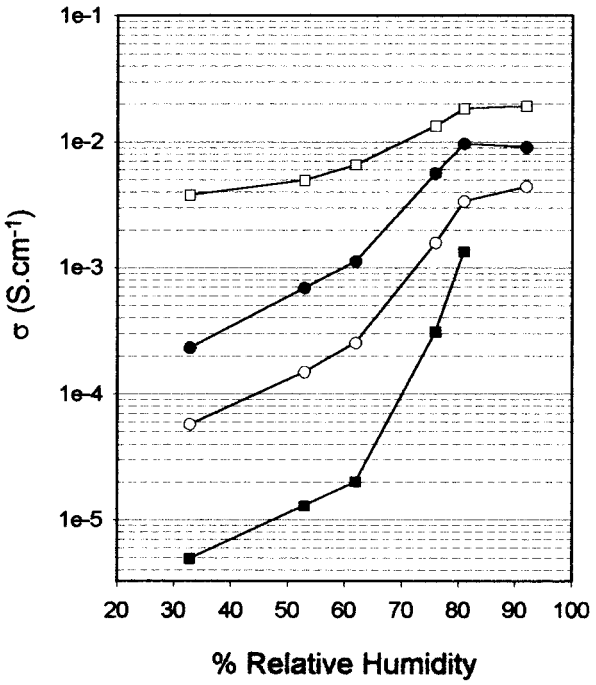

Figure 7. Effect of RH on the proton conductivity of Ti400 (■), TiP4.0 (○), TiP2.5 (●), and Ti1.5 (□).

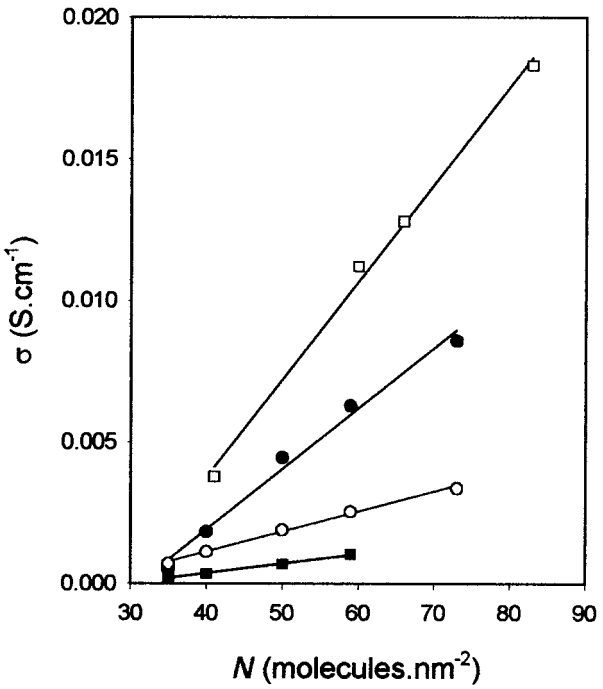

Figure 8. Effect of water content (*N*) on the proton conductivity of Ti400 (■), TiP4.0 (○), TiP2.5 (●), and Ti1.5 (□).

the fact that the surface site density of five-coordinated Ti^{4+} sites (5.4/nm^2), to which phosphate ions are thought to coordinate, is 7.6 times larger than the loading density of phosphate ions. Assuming that phosphate ions form monodentate complexes on the surface, H_2O/OH groups could outnumber the phosphate ions by 15 to 1, or by half this ratio if the surface complexes were bidentate. These preliminary results on phosphated samples are encouraging and make it worthwhile to investigate the preparation of samples with larger phosphate loading.

Effect of Relative Humidity. The conductivities of all materials in this study increased with increasing RH. In this regard, the materials behave as typical protonic conductors. The conductivity versus relative humidity curve for Nafion 117 has a different shape than the ones shown by our materials (Figure 7). Curves in Figure 7 are S-shaped, while Nafion 117, in the same range of RH (30 to 80%) presents either a linear[2] or exponential[5] behavior.

The plots in Figure 7 show that the influence of RH on conductivity varies greatly from one material to another. The conductivity of Ti1.5 changes less than 1 order of magnitude when the RH increases from 30 to 90%. Meanwhile, the same change in RH causes the conductivity of Ti400 to increase more than 2 orders of magnitude. Furthermore, the difference in conductivity among these samples is 3 orders of magnitude at RH below 60%, whereas at RH above 80% the difference is of only 1 order of magnitude.

The large difference in conductivity among these four materials can be attributed to their unequal water adsorption behavior, which was previously illustrated in Figure 2. For example, at 30% RH value of *N* for Ti1.5 is 1.8 times larger than that of Ti400; at 90% RH the former still has 1.3 times the water of the latter. While the unequal water adsorption behavior of these samples should lead to differences in their conductivity values at a given RH, this may not be the only property of the materials generating such differences in conductivity.

As demonstrated in Figure 8, the conductivities of samples Ti400, TiP4.0, TiP2.5, and Ti1.5 show a linear response to changes in their water content. The rate of change, $\Delta\sigma/\Delta N$, is different for each sample, and increases in the order Ti400 < TiP4.0 < TiP2.5 < Ti1.5. The fact that these samples have different conductivities for the same *N* forces us to reason that the nature of the pore water is different for each sample. Variations in conductivity for a constant *N* should be associated with differences in the concentration of H^+ in the pore water, and also with potential differences in the mobility of the protons. Specifically, variations in proton mobility of samples Ti400 and Ti1.5 can be caused by differences in the surface site density and in the surface charge. The expected unequal conductivity at a given *N* between phosphated and non-phosphated samples will have additional sources, namely, differences in the surface pK_a and changes in the structure of the first few layers of physisorbed water due to the presence of hydrated phosphate ions. The state of polarization of the water molecules hydrating the surface phosphate as well as their orientation in relation to the pore wall are expected to be different than that of the water hydrogen bonded to surface H_2O^+/OH groups.

For $N = 60$ molecules/nm^2, one-third of the water in the Ti400 sample can be described as forming part of the layer of water clusters (interfacial water) (see Figure 2), while the other two-thirds are associated with capillary condensation and therefore can be regarded as water having bulk character. On the other hand, two-thirds of the water in the Ti1.5 sample should be labeled as interfacial and one-third as bulk. The net result is that the conductivity of Ti1.5 is 1 order of magnitude larger than the one of T400.

The dependence of conductivity on water content for polymeric membranes such as Dow and Nafion has been

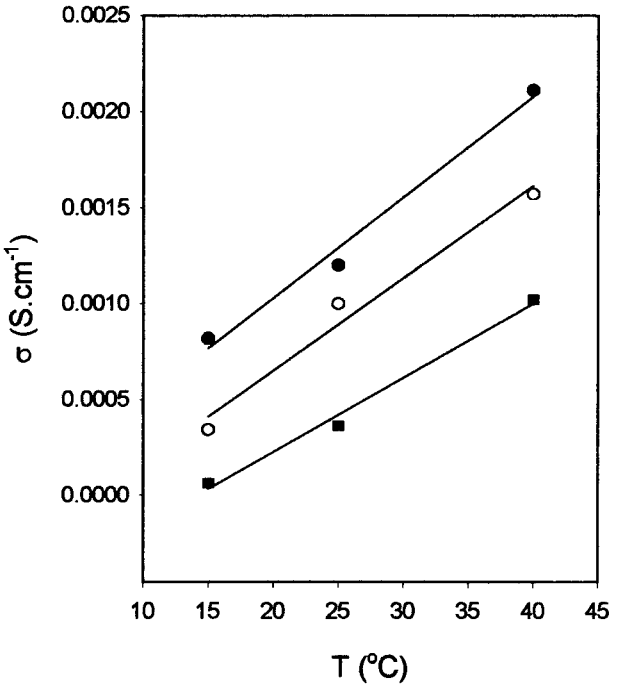

Figure 9. Temperature dependence of conductivity for materials with a $N = 40$ molecules/nm^2: Ti400 (■), TiP4.0 (○), and TiP2.5 (●).

described in the literature as a two regime phenomenon. Below 5 (Dow) and 4 (Nafion) molecules of water/sulfonic group (approximately at 58% RH) the conductivity increases exponentially with water content. In the region of higher hydration the conductivity has a linear dependency.[1] In the case of our materials, we have always found a very good linear response of conductivity versus water content in the range of hydration studied (RH between 30% and 90%).

Effect of Temperature. The conductivities of our materials increase with temperature in the range of 15−40 °C, regardless of N. The relation between conductivity and temperature at a constant N for some of these materials is illustrated in Figure 9. In every case studied, conductivity shows an Arrhenius-like dependence with temperature. The Arrhenius equations for samples Ti400, TiP4.0, TiP2.5, and Ti1.5, showing the linearity of these plots, are presented in Table 3.

In all four samples, the activation energy for proton mobility (E_a) is dependent on N, as shown in Figure 10, and can be described as a three regime phenomenon. The activation energy first falls, and then rises with increasing N. At still higher states of hydration, the activation energy becomes almost independent of N. The E_a versus N curves of all four samples qualitatively resemble each other. However, the E_a for a given value of N is different for each sample. The highest and lowest values for E_a are connected with samples Ti400 and Ti1.5, respectively. Incidentally, these two materials also are associated with the lowest and highest values of conductivity, respectively.

The value of N at the minimum of each of these curves coincides with the water content at the starting point for capillary condensation in the corresponding water adsorption isotherm (see Figure 2). Thus, values of E_a connected to N smaller than that of the minimum in the curve should be attributed to proton motion in the

Table 3. Equation Parameters for Arrhenius Plots: Equation: $\log \sigma = (1/T)a + b$

	N (H_2O/nm^2)[a]	E_a (kJ mol^{-1})	a	b	R^2
Ti400	19	39.3	−2051.1	1.6644	0.9941
	25	24.5	−1280.8	−0.3909	0.9898
	30	51.3	−2680.0	4.7707	0.8171
	35	75.3	−3932.4	9.3048	0.8726
	40	81.8	−4272.6	10.723	0.9429
Ti1.5	40	20.6	−1073.6	0.5629	0.9606
	44	16.8	−879.19	0.3290	0.9985
	50	35.3	−1845.7	3.8554	0.9948
	60	42.9	−2238.6	5.3388	0.9996
	70	38.3	−2002.3	4.7062	0.9788
TP2.5	35	29.9	−1559.7	1.7847	0.9990
	40	28.8	−1502.2	2.1091	0.9854
	50	36.5	−1908.7	3.7407	0.8736
	55	38.1	−1990.7	4.1956	0.8760
	60	37.0	−1934.5	4.1376	0.9300
TP4.0	30	30.6	−1597.7	1.5606	0.9920
	35	33.6	−1755.6	2.5008	0.9245
	40	44.0	−2297.2	4.5953	0.8554
	45	46.2	−2413.8	5.1873	0.9249
	50	46.5	−2427.2	5.3683	0.9765

[a] Physisorbed water as determined from the adsorption isotherms.

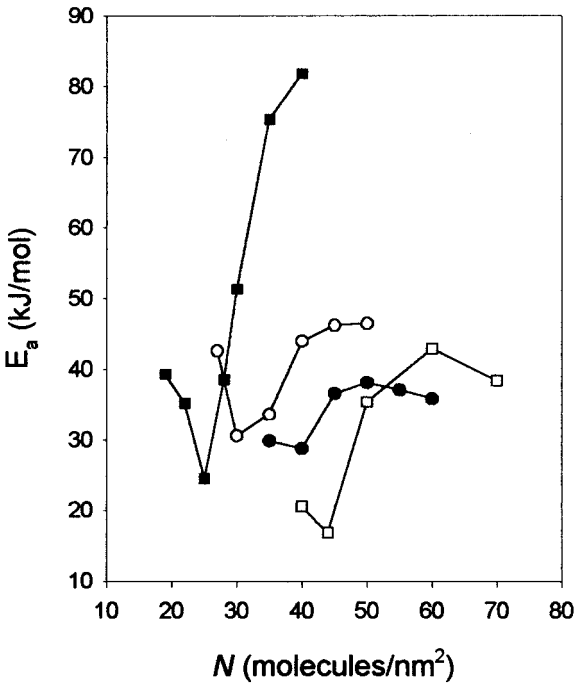

Figure 10. Effect of water content (N) on the proton mobility activation energy of Ti400 (■), TiP4.0 (○), TiP2.5 (●), and Ti1.5 (□).

layer of interfacial water. E_a values at higher N should be influenced by both the proton motion in the interfacial water layer and proton motion in the bulklike water filling the pores. Adsorption of additional water molecules in the cluster layer (compare Figures 2 and 10) decreases the activation energy. When the newly adsorbed water molecules start filling the pore space by forming bridges between the hydrated pore walls, the average activation energy increases.

Activation energies of proton mobility in the interfacial water are larger for the Ti400 sample than for the Ti1.5. This result can be explained on the grounds of existing differences in some of the physicochemical properties of these samples. The density of sites to which

the water can adsorb is 11.4 sites per square nanometer for Ti1.5 versus 10.2 per square nanometer for Ti400. Moreover, the number of water molecules associated with each of these sites is 3.9 for Ti1.5 versus 2.4 for Ti400. As a consequence, the water clusters in the interfacial layer of water of Ti1.5 should be closer to each other than those in the interfacial layer of Ti400. Therefore, proton hopping along the interfacial layer of water will be easier in the case of sample Ti1.5; and, according to the literature,[19] at this level of surface hydration proton conduction occurs mainly through a Gröttus-type mechanism. However, the distance between molecules in different water clusters may not be the only explanation for the difference in the activation energy. It is known that the structure of water (orientation and hydrogen bond strength) in the cluster influences the activation energy of proton hopping.[21,28] The Ti400 and Ti1.5 samples are expected to contain clusters having different water structure since the latter has a much more positive surface charge than the former.

In some instances, the structure of water in the clusters may be more influential than the distance between water molecules. As Figure 10 shows, although both site density and number of water molecules per site are higher for TiP2.5 than for Ti400, the activation energy associated with the interfacial water layer is larger for sample TiP2.5 than for Ti400.

By comparison, activation energy for proton mobility in Nafion ranges from 17 to 29 kJ mol^{-1}.[1,4,22] Activation energies for proton hopping in dehydrated zeolite H−ZSM5 range from 89 to126 kJ.mol^{-1}, depending on the SiO_2/Al_2O_3 ratio.[19] England and co-workers[29] report activation energies of 33.8 and 23.2 kJ.mol^{-1} between 0 and 40 °C for hydrous ZrO_2 and SnO_2, respectively. The proton-transfer activation energy for $H_3PW_{12}O_4 \cdot 0.29H_2O$ is 19 kJ mol^{-1}.[28] Depending on the proton concentration, the activation energy ranges from 10.9 kJ mol^{-1} in pure water (activation energy to break a hydrogen bond between water molecules) to almost 19 kJ mol^{-1} in protonated water (activation energy to break the hydrogen bond with a hydronium ion[21]). The activation energy for proton motion in our materials ranges between 15 kJ mol^{-1} (interfacial water) and 85 kJ mol^{-1} (interfacial water + water in partially filled pores) and is therefore higher than that observed in pure water.

Conclusions

The surface chemistry of the pore walls of mesoporous TiO_2 wafers is a determining factor in the water adsorption behavior of these materials. The uptake of physisorbed water is a two-regime process. At lower RH the water forms a layer of clusters along the walls (interfacial layer) of a matrix of interconnected pores. At higher RH new water molecules start filling the remaining pore space through capillary condensation. The capacity of the interfacial layer of water is strongly influenced by the chemistry of the pore wall. However, uptake by capillary condensation is independent of the surface chemistry of the pore wall. Therefore, the pore water density is different for each of the studied materials, and in every case larger than that of water at 40 °C.

The proton conductivity values for these materials increases with increasing water content. Moreover, In the first regime of hydration, the activation energy decreases with increasing water content, whereas in the capillary condensation regime, activation energy increases, to a limit, with increasing water content. Although differences in the proton conductivity of these materials are related to their differences in water adsorption behavior, the values for proton conductivity do not totally correlate with the water content of a sample. This indicates existing differences in both proton concentration and proton mobility in the pore water.

Acknowledgment. F.M.V. wishes to acknowledge FAPESP for the grant conceded. This work is funded by the US Department of Energy under contract DE-FC02-99EE50583.

CM9907460

(28) Yaroslavtsev, A. B.; Gorbatchev, D. L. *J. Mol. Struct.* **1997**, *416*, 63.
(29) England, W. A.; Cross, M. G.; Hamnett, A.; Wiseman, P. J.; Goodenough, J. B. *Solid State Ionics* **1980**, *1*, 231.